Damping in roll tests of a 1/120 scale model of the CF-105 aircraft

LaBerge, J. G.

Publisher's version / Version de l'éditeur:
https://doi.org/10.4224/23000747
Laboratory Memorandum (National Research Council of Canada. National Aeronautical Establishment. Aerodynamics); no. AE-46(o), 1958-06-12

(L. O. Copy) Templin

L.O. NAE-586	**NATIONAL AERONAUTICAL ESTABLISHMENT**	HSAL-M-111
FILE M2-1-86	OTTAWA, CANADA	NO. AE-46(o)
PREPARED BY JGL	LABORATORY MEMORANDUM	PAGE 1 OF
CHECKED BY KOR	SECTION Aerodynamics	COPY NO. 4
		DATE 12 June 1958

DECLASSIFED on August 29, 2016 by Steven Zan.

Initial

SECURITY CLASSIFICATION ~~Confidential~~

SUBJECT Damping in Roll Tests of a 1/120 Scale Model of the CF-105 Aircraft

PREPARED BY J. G. LaBerge

ISSUED TO
Dr. D. C. MacPhail
Mr. J. H. Parkin
Mr. R. J. Templin (2)
Mr. K. Orlik-Rückemann (2)
Author
Aero Library (2)

THIS MEMORANDUM IS ISSUED TO FURNISH INFORMATION IN ADVANCE OF A REPORT. IT IS PRELIMINARY IN CHARACTER, HAS NOT RECEIVED THE CAREFUL EDITING OF A REPORT, AND IS SUBJECT TO REVIEW.

List of Symbols

I - moment of inertia of the oscillating system, Lb.In.Sec.^{2}

T_o - stagnation temperature, °K

p_o - stagnation pressure, mm Hg

δ - logarithmic decrement

δ_o - logarithmic decrement in vacuum

ν - oscillation frequency, Cycles/Sec.

ν_o - oscillation frequency in vacuum, Cycles/Sec.

K - spring constant of test rig, Lb.In./Rad.

b - wing span of model, 5.00 in.

S - wing area of model, 12.25 in.^{2}

γ - ratio of specific heats, C_p/C_v

R - gas constant, 96 Ft.Lb./Lb.°K

1.0 Introduction

In order to assess the performance of the new oscillation-in-roll test rig a 1/120 scale model of the CF-105 aircraft was tested on it in the 30 in. wind tunnel at subsonic and supersonic speeds. For low supersonic speeds the results were compared with those of AVRO free flight model tests and CARDE aeroballistic range tests.

2.0 Wind Tunnel

Supersonic Mach numbers were achieved by exchanging solid magnesium liners while subsonic Mach numbers were obtained by varying the flexible diffuser throat with the M=1.22 nozzle block permanently in place. At subsonic and low supersonic speeds, pressure measurements were made along the floor of the tunnel extending from 4.5 mean aerodynamic chords upstream to 4.8 downstream of the model. These served to verify the uniformity of flow over the model and to determine the Mach number at subsonic speeds. At the latter speeds the Mach number distributions were uniform to better than $\pm 0.5\%$ while at supersonic speeds this figure was about $\pm 0.7\%$.

The tunnel intake air, at approximately atmospheric pressure and temperature, was dried to a specific humidity of less than 0.0005.

3.0 Test Rig

The model was mounted on a sting-type test rig (to be described in a forthcoming memorandum) in such a way that it could move elastically in roll and was rigidly restricted in the other degrees of freedom. The test rig also contained an electromagnetic oscillator by means of which the desired oscillations in roll could be imparted to the model. Amplitudes of $\pm 3°$ could be obtained at the natural frequency of the oscillating system.

The spring constant, determined by loading the test rig statically in roll and measuring the deflections, is given in Figure 1. The moment of inertia of the oscillating system is then found from

$$I = \frac{K}{4\pi^2 \nu_o^2}$$

The test rig was mounted on a horizontal support bar which spanned the tunnel at the diffuser entry. The size of the bar as well as the method of attachment to the side walls was such that a very rigid support for the test rig was provided at the same time keeping the blockage area to a minimum. The support bar could be rotated about its axis to vary the model angle of attack in the range from -3° to +15° in steps of 1°. A groove along the top surface of the bar allowed the balance electrical wires to be led out through a suitable hole in the side wall of the tunnel.

4.0 Test Model

The test was done with a standard* model used in the CARDE aero-ballistic range, modified by CARDE for sting mounting. The modification involved a change in the duct exit configuration so that the latter blended into a cylindrical extension to fit the test rig. Due to the small scale of the model the intake ducts were left solid; hence the tests were conducted under the condition of no duct mass flow.

The model mounted in the tunnel is shown in Figure 2 while the geometric details are given in Figure 3.

---

* But made of steel for the tunnel tests.

5.0 Test Method

The tests were performed using the method of free oscillations with feedback excitation. The block diagram of the instrumentation used is given in Figure 4. The tests were carried out by imparting to the model an initial oscillation of a desired amplitude, disconnecting the feedback loop and recording the characteristics of the resulting decaying oscillations on the Dampometer.

A multi-tube mercury manometer was used to determine the static pressure distribution along the tunnel floor.

6.0 Test Procedure

In the wind off condition, i.e., before and after each tunnel run, ten readings of the damping and frequency were taken so as to form a wind off average. Tunnel runs of about 15 seconds duration were taken during each of which 5 measurements of the damping and frequency could be obtained. In general 3 tunnel runs were made for each data point so that up to 15 values of the damping and frequency were available for averaging.

Inasmuch as the damping and frequency were required in vacuum, readings (ten) were taken with the tunnel working section at a small absolute pressure from which it was possible to extrapolate to zero pressure, as indicated in Figure 5. The frequency was found to vary little under vacuum, wind off and wind on conditions, its value being about 265 cycles per second, which corresponds to a reduced frequency

$$k = \frac{2\pi \nu b}{2V} = 0.24 \text{ at } M = 1.57.$$

The damping and frequency values obtained were representative for the amplitude range 0.4° to 1.2°.

Boundary layer transition on the model was natural and probably took place well aft on the wing, as indicated by the results of previous measurements on a slightly larger scale model of the same aircraft.

The Mach number range extended from 0.42 to 0.84 and from 1.46 to 2.03.☆ The corresponding Reynolds number varied from 0.66 to 0.96 based on the wing mean aerodynamic chord.

The extent of the test programme, in terms of Mach number and angle of attack, is given in Table I.

7.0 Data Reduction

The damping-in-roll derivative was computed in a manner similar to that of Reference 1, section 4, and is

$$-C_{\ell_p} = \frac{8I}{\rho V S b^2} \left(\delta \nu - \delta_o \nu_o \right) \qquad (1)$$

The term ρV was found from

$$\rho V = \left(\frac{\rho V}{\rho_o a_o} \right) \rho_o a_o = \frac{\rho V}{\rho_o a_o} \sqrt{\frac{\gamma}{R}} \quad \frac{p_o}{\sqrt{T_o}} = f(M) \frac{p_o}{\sqrt{T_o}}$$

whence

$$-C_{\ell_p} = \frac{8I}{Sb^2} \, \frac{1}{f(M)} \, \frac{\sqrt{T_o}}{p_o} \left(\delta \nu - \delta_o \nu_o \right)$$

$$= H(M) \frac{\sqrt{T_o}}{p_o} \left(\delta \nu - \delta_o \nu_o \right) \qquad (2)$$

The factor H (M) which, for a given model, is a function of only the Mach number, is given in Table II.

☆ The transonic range was excluded due to blockage produced by the support bar.

8.0 Accuracy of Results

As in Reference 1, it was found that errors in δ_o, ν and ν_o were negligible compared to the error in δ. The standard deviation $\bar{\sigma}$ of the arithmetic mean value of the damping-in-roll derivative was found from the expression

$$\bar{\sigma} = \left[\frac{\sum_{t=1}^{n} \left(C_{\ell_{p_t}} - C_{\ell_p} \right)^2}{n(n-1)} \right]^{\frac{1}{2}}$$

where $C_{\ell_{p_t}}$ is the t^{th} measurement, C_{ℓ_p} is the mean value and n the number of measurements. The values of $\bar{\sigma}$ as well as the total scatter of the data are given in Table I.

9.0 Discussion of Results

The damping-in-roll derivative is plotted against Mach number in Figure 6. It will be noted that the variation with Mach number over the Mach number range tested is not very great. For comparison, the results of two tests with 1/8 scale free flight models, as reported in Reference 2, have been included. In addition, the results of tests conducted in the aeroballistic range using a 1/120 scale model are shown.

It will be seen that at low supersonic speeds the agreement appears to be reasonable. However, no further direct comparison can be made since most of the free flight tests were carried out in the transonic range.

The effect of angle of attack on the tunnel results is indicated in Figure 6.

The results reported herein have not been corrected for wing flexibility. However, in another series of tests at supersonic speeds using other models it was found that the damping-in-roll derivative for steel delta wings was about 5% smaller than that for rigid wings at similar frequencies.

10.0 Conclusions

Subsonic and supersonic wind tunnel tests on a 1/120 scale model of the CF-105 aircraft have shown that the damping-in-roll derivative was relatively insensitive to Mach number and for zero angle of attack was close to -0.25 in the speed ranges investigated. The variation of angle of attack within the range 0°-10° could change this value (usually by increasing it) by an amount smaller than 25%.

Free-flight model tests and aeroballistic range tests gave results of the same order of magnitude as those obtained in the wind tunnel at low supersonic Mach numbers, where the speed range of the various facilities coincided.

Throughout the test programme the damping-in-roll test rig performed satisfactorily and its design can be considered successful.

References

1. K. Orlik-Rückemann and C. O. Olsson — A Method for the Determination of the Damping-in-Pitch of Semi-Span Models in High-Speed Wind-Tunnels, and Some Results for a Triangular Wing. The Aeronautical Research Institute of Sweden, FFA, Report No. 62, 1956.

2. M. V. Jenkins — CF-105 Free Flight Stability Model Results. A.V. Roe Canada Ltd. Rep. No. P/FFM/57, July 1957.

JGL/JVT

Table I

Summary of Results

M	α Degrees	C_{l_p}	$\bar{\sigma}$	Total Scatter
0.421	0	0.234	±0.002	+0.008 -0.009
0.475	0	0.234	±0.001	+0.004 -0.005
	5	0.287	±0.002	+0.007 -0.007
	10	0.301	±0.002	+0.008 -0.008
0.592	0	0.234	±0.002	+0.014 -0.011
0.664	0	0.245	±0.004	+0.016 -0.020
	5	0.312	±0.003	+0.012 -0.014
	10	0.295	±0.004	+0.024 -0.015
0.748	0	0.252	±0.003	+0.014 -0.008
0.802	0	0.244	±0.002	+0.009 -0.011
0.840	0	0.242	±0.003	+0.016 -0.009
1.46	0	0.261	±0.002	+0.011 -0.009
	5	0.283	±0.002	+0.011 -0.008
	10	0.249	±0.001	+0.007 -0.009
1.57	0	0.257	±0.001	+0.007 -0.007
1.78	0	0.254	±0.003	+0.015 -0.012
2.03	0	0.227	±0.004	+0.008 -0.014
	10	0.185	±0.002	+0.005 -0.011

Table II

Mach Number Function

M	H (M)
0.421	2.594
0.475	2.365
0.592	2.037
0.664	1.910
0.748	1.809
0.802	1.764
0.840	1.741
1.46	1.955
1.57	2.086
1.78	2.410
2.03	2.942

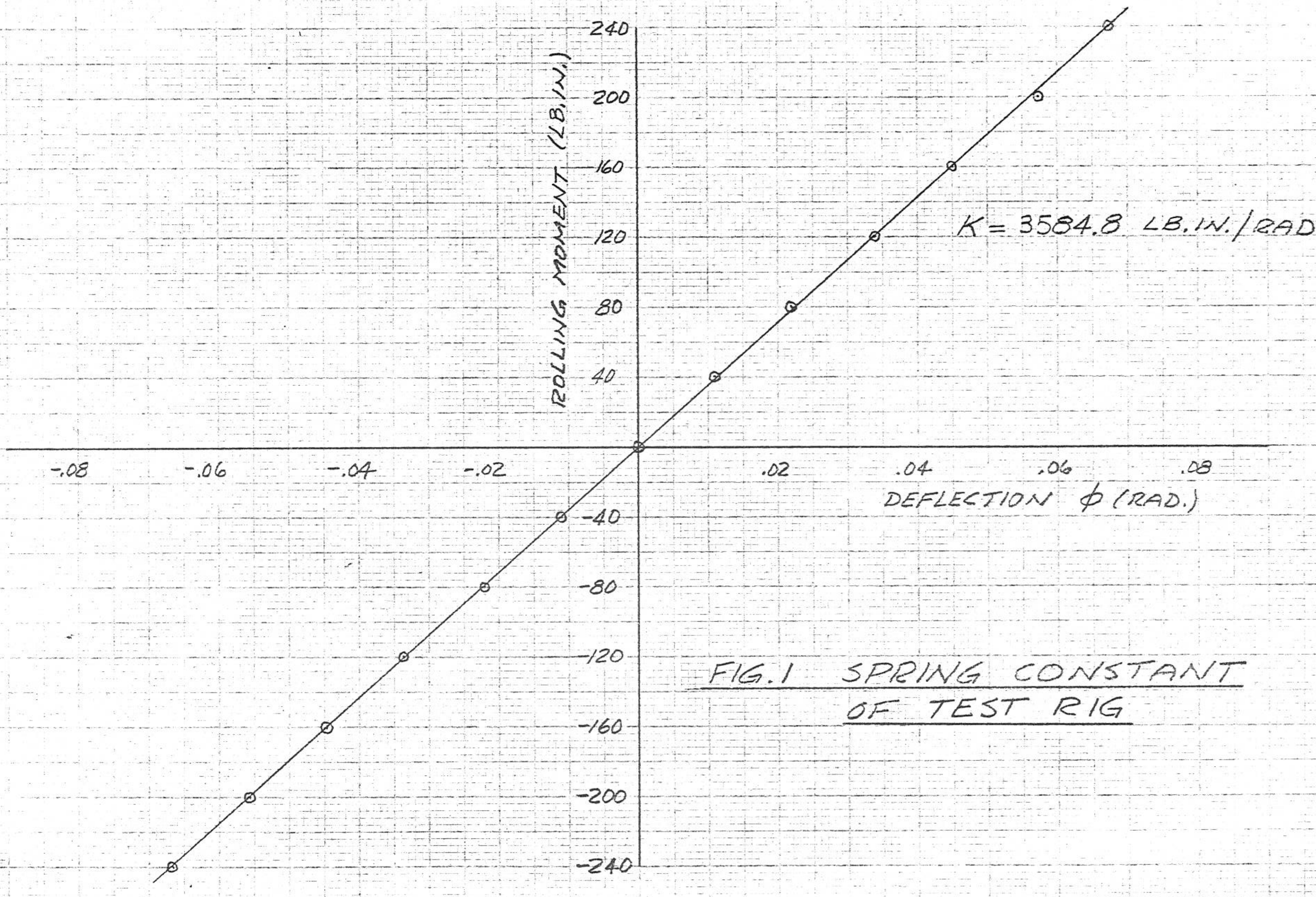

FIG. 1 SPRING CONSTANT OF TEST RIG

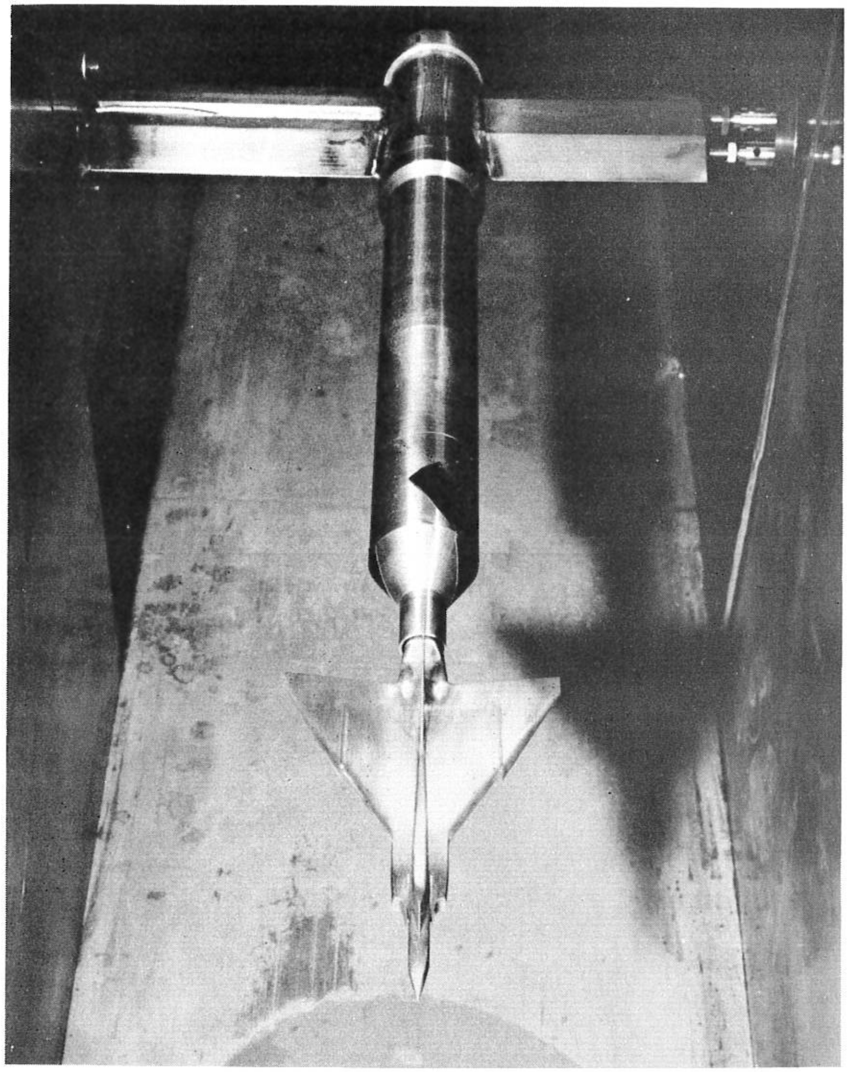

FIG. 2 TEST MODEL MOUNTED IN TUNNEL

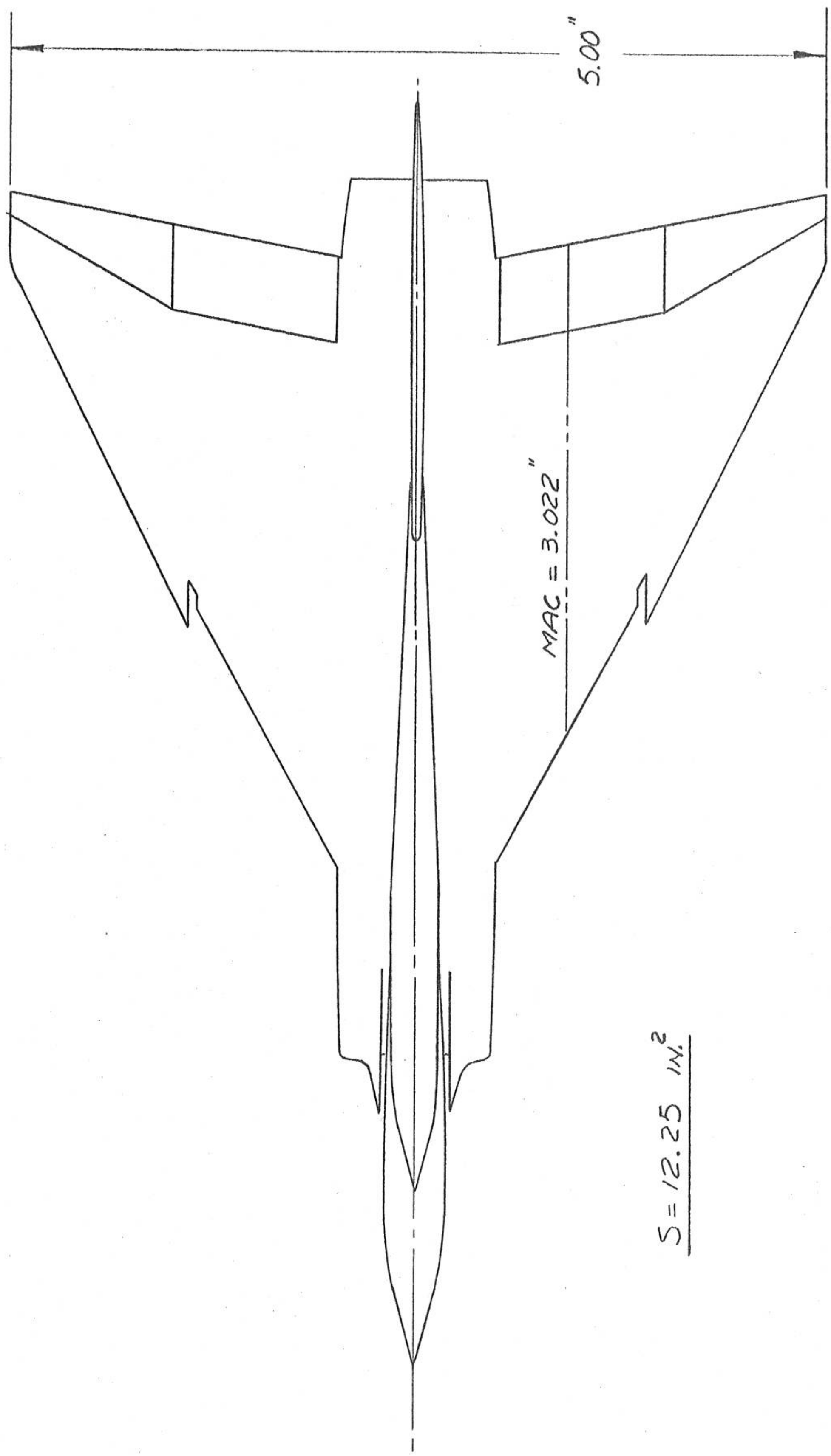

FIG. 3 DIAGRAM OF TEST MODEL

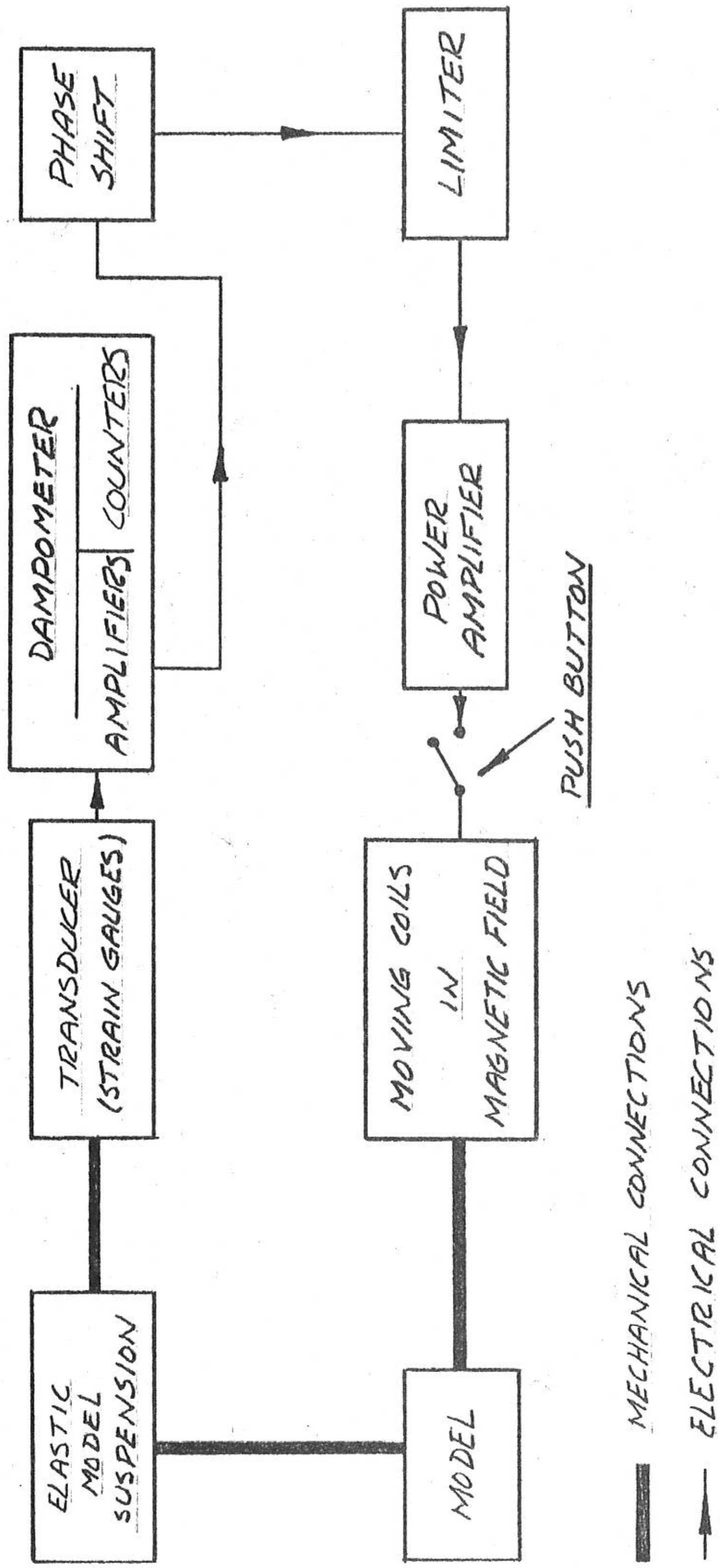

FIG. 4 DIAGRAM OF INSTRUMENTATION

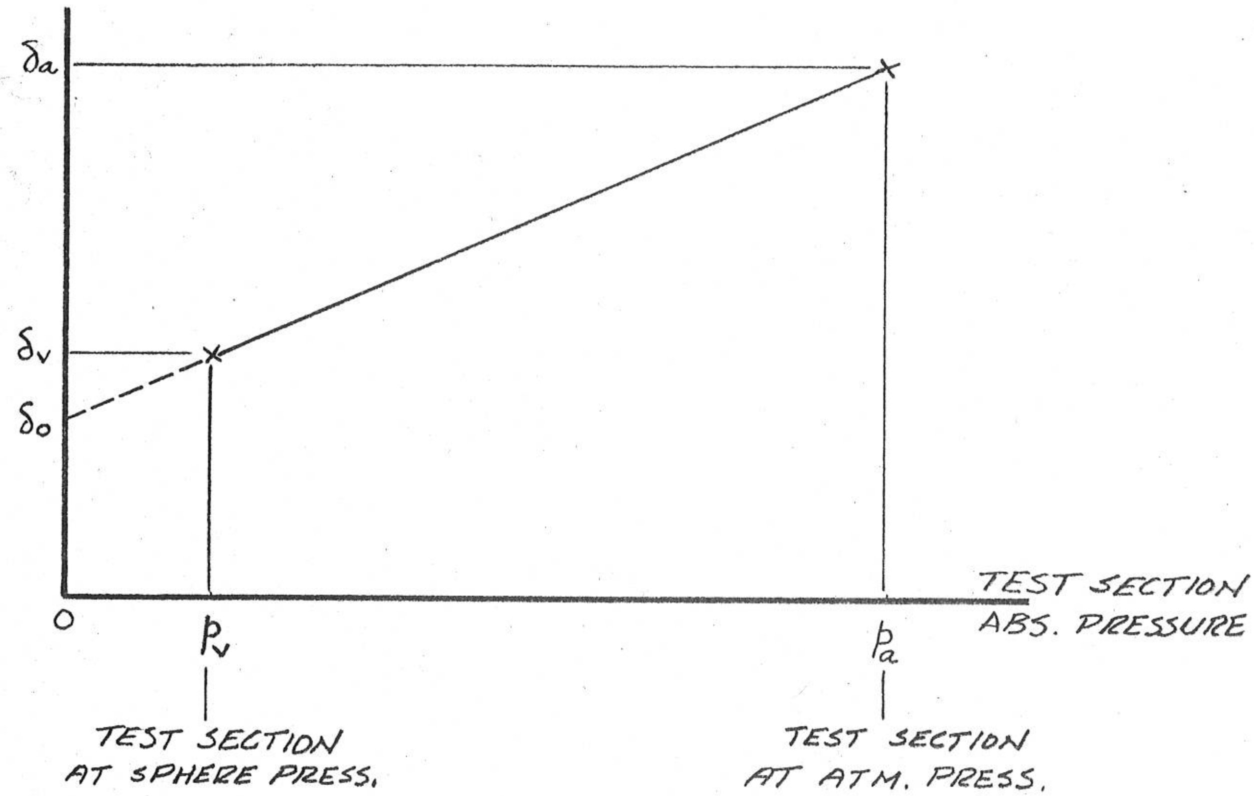

$$\delta_o = \frac{\frac{p_a}{p_v}\delta_v - \delta_a}{\frac{p_a}{p_v} - 1}$$

WHERE

$(\ )_o$ STANDS FOR ZERO ABSOLUTE PRESSURE

$(\ )_v$ STANDS FOR SPHERE PRESSURE

$(\ )_a$ STANDS FOR ATMOSPHERIC PRESSURE

FIG. 5 LOGARITHMIC DECREMENT AT ZERO ABSOLUTE PRESSURE

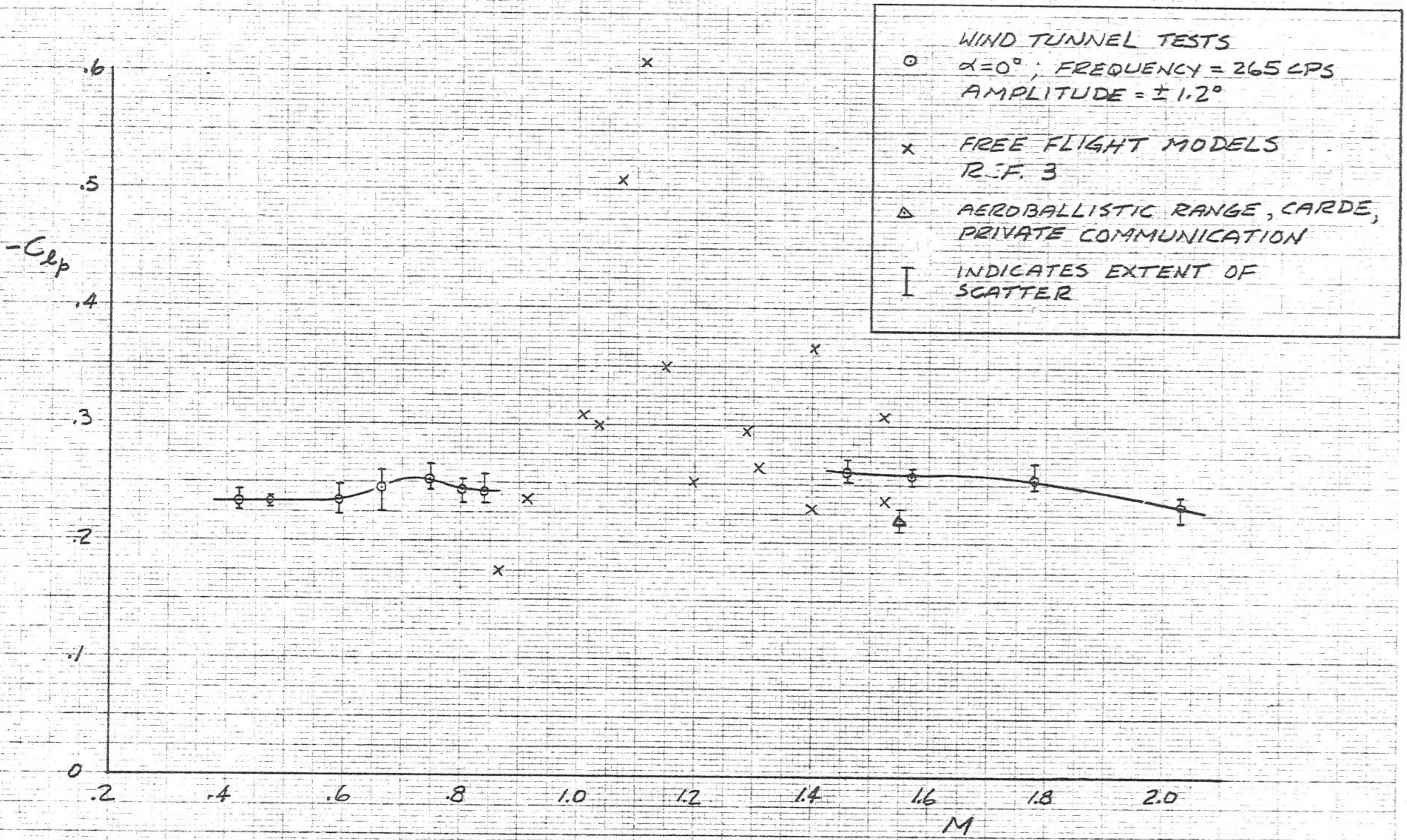

FIG. 6 C_{l_p} VS MACH NUMBER

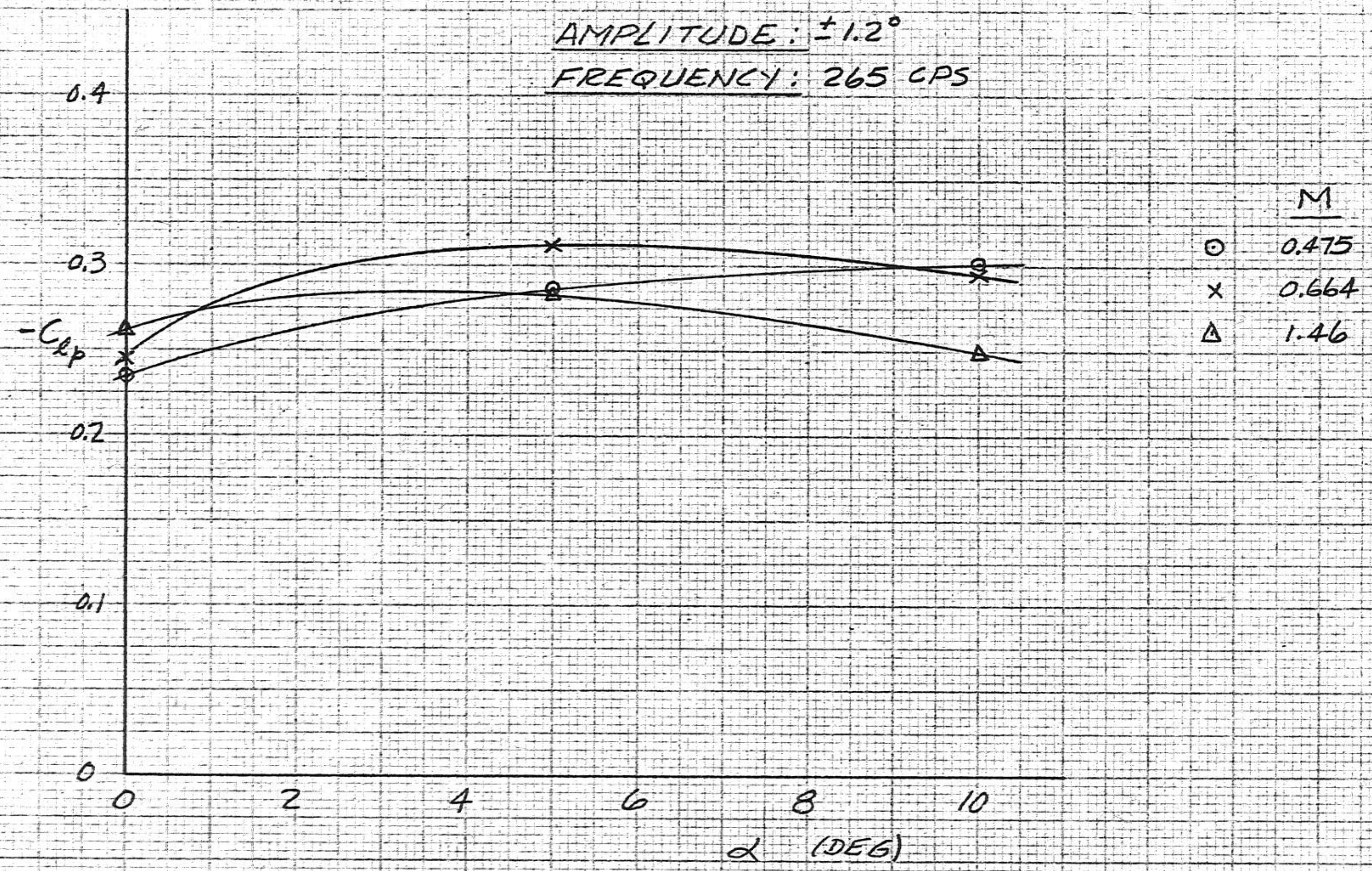

FIG. 7 C_{l_p} VS ANGLE OF ATTACK